ROBUST DESIGN OF A POWER SYSTEM STATCOM CONTROLLER USING LOOP-SHAPING TECHNIQUE

A. H. M. A. Rahim[1] and M. F. Kandlawala[1]

Department of Electrical Engineering, KFUPM

Email: ahrahim@kfupm.edu.sa

ABSTRACT

A Static synchronous compensator (STATCOM) is one of the new generations of flexible AC transmission system (FACTS) devices with promising features of applications in power system. STATCOMs are used to stabilize the system by exchanging reactive power in the power system. In this article, dynamic behavior of a single machine infinite bus power system with STATCOM has been investigated. A 5th order dynamic model is considered. The effect of PID control in damping enhancement has been investigated. It has been found that the gains of the PID controller need to be retuned with the change in the operating conditions. In order to overcome this, a robust STATCOM damping controller has been proposed. The design is carried out applying robustness criteria for stability and performance. A loop-shaping technique has been employed to select a suitable open-loop transfer function, from which the robust controller is constructed. The proposed controller has been tested through a number of disturbances including three-phase faults. The robust controller has been demonstrated to provide satisfactory damping characteristics over a good range of operating conditions

Keywords: *Power System, FACTS, STATCOM, Damping Control, PID control, Loop-shaping method, Robust Control.*

الملخص

يعد المعادل المتزامن الثابت (STATCOM) أحد أنظمة الجيل الجديدة والمرنة لنقل التيار المتردد FACTS والتي تبشر بتطبيقات متعددة في مجال الطاقة. تستخدم STATCOMS لتثبيت النظام عن طريق تبادل الطاقة الترجعية مع نظام الطاقة. في هذه الرسالة تم بحث السلوك النشط لنظام طاقة لماكنية أحادية ذات ناقل لا متناهي مع STATCOM. وتم إستخدام نموذج رياضي مفصل من الدرجة الخامسة لتحسين المضائلة. ولوحظ تأثير PID التحكم بالمضائلة لنظام الطاقة فوجد أن تضخيم المتحكم PID يحتاج إلى تعديل حسب التغير في حالات التشغيل, ولتغلب على هذه المشكلة تم أستخدام STATCOM متين للتحكم بالمضائلة. نفذ التصميم بإستخدام معايير ثبات وقوي للإستقرار والأداء تم تقديم تصميم STATCOM لمضائلة كهروميكانيكية عابرة وتغيرات الفولتية لاذو ثبات قوي من أجل محاكاة التغيرات في نقاط التشغيل في النظام ، وتم إستخدام STATCOM لضبط طريقة الشك المضاعف.. وتم تطبيق تقنية تشكيل العقد لإنتقاء دالة النقل المناسبة والتي تم من خلالها بناء مضبط ذو ثبات عالي. تم عرض كيفية استخدام هذا المضبط ذو الثبات العالي لإعطاء ميزات مضائلة جيدة جدا على تشكلية واسعة من ظروف التشغيل.

1. INTRODUCTION

Reactive power compensation is known to increase the power transmission in AC lines. Fixed or mechanically switched capacitors and reactors have long been employed to increase the steady-state power transmission by controlling the voltage profile along the lines [Gyugi, 1994]. Controllable synchronous voltage sources known as static synchronous compensators are a recent introduction in power system for dynamic compensation and for real time control of power flow. The static synchronous compensator (STATCOM) provides shunt compensation in a way similar to the static VAR compensators (SVC), but utilizes a voltage source converter rather than shunt capacitors and reactors [Machowaski, 1997]. STATCOM is an active device, which can control voltage magnitude and phase in a very short time and therefore has the ability to improve the system damping as well as voltage profiles of the system. It has been reported that STATCOM can offer a number of performance advantages for reactive power control applications over the conventional SVC because of its greater reactive current output at depressed voltage, faster response, better control stability, lower harmonics and smaller size, etc. [Wang, 1999]

Two basic controls are implemented in a STATCOM [Li, 1998; Wang, 1999]. The first is the AC voltage regulation of the power system, which is realized by controlling the reactive power interchange between the STATCOM and the power system. The other is the control of the DC voltage across the capacitor, through which the active power injection from the STATCOM to the power system is controlled [Li, 1998; Wang, 2000]. The effect of stabilizing controls on STATCOM controllers have been investigated in several recent papers [Li, 1998; Wang, 1999; Wang, 2000; Padiyar et al, 1996].

A single machine infinite-bus system with a long transmission network with STATCOM connected at the middle of the line has been considered in this study. Two controls for the STATCOM have been identified. One is the magnitude and the other is the phase angle of the STATCOM voltage. Implementing different combinations of PID controller, the effectiveness of the STATCOM voltage magnitude control strategy has been tested. Simulation results show that suitably designed PID controllers can provide good damping, but will not operate satisfactorily over a wide range of operating conditions. To overcome the difficulties of the PID controller a robust design procedure for the STATCOM voltage magnitude control has been considered. A loop-shaping technique has been employed for the robust controller design. The robust controller designed was tested over a range of operating conditions for a number of disturbances. The controller was found to be effective in providing good damping characteristics over a wide range of operating conditions.

2. SINGLE MACHINE INFINITE BUS MODEL WITH STATCOM

A single machine infinite bus system with STATCOM installed at the middle of the transmission line is shown in Fig. 1. The system consists of a step down transformer (SDT) with a leakage reactance X_{SDT}, a three phase GTO–based voltage source converter (VSC), and a DC-capacitor. The STATCOM is modeled as a voltage sourced converter behind a step down transformer. The VSC generates a controllable AC-voltage source $v_o(t)=V_o \sin(\omega t-\Psi)$ behind the leakage reactance. The active and reactive power exchange between the STATCOM and the power system can be controlled by adjusting the magnitude V_o and the phase Ψ of the STATCOM voltage.

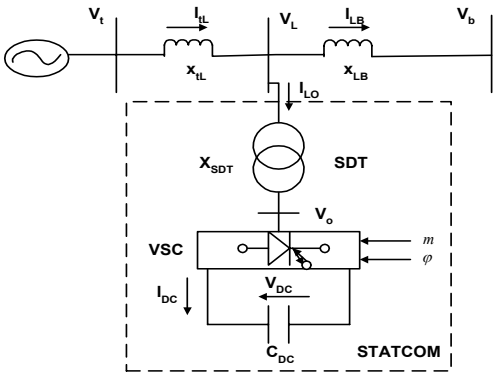

Fig.1 Single machine infinite bus power system configuration with STATCOM

From Fig.1, the voltage current relationships of the STATCOM are expressed as [Wang, 1999],

$$\bar{I}_{Lo} = \bar{I}_{Lod} + j\ \bar{I}_{Loq}$$

$$V_o = eV_{DC}\left(\cos\psi + j\sin\psi\right) = eV_{DC}\angle\psi \qquad (1)$$

$$\frac{dV_{DC}}{dt} = \frac{I_{DC}}{C_{DC}} = \frac{e}{C_{DC}}\left(I_{Lod}\cos\psi + I_{Loq}\sin\psi\right)$$

where, e = mk, k is the ratio of AC / DC voltage, m is the modulation ratio defined by PWM, and Ψ is phase angle defined by PWM.

From (1), it can be seen that the magnitude of the STATCOM voltage V_{DC} depends on 'e', which is a measure of the magnitude of the STATCOM output voltage. The nonlinear dynamic model of the generator including the STATCOM is written as,

$$\dot{\delta} = \omega_o \Delta\omega$$

$$\dot{\omega} = -\frac{1}{M}\left[P_m - P_e - D\Delta\omega\right]$$

$$\dot{e}_q^{'} = \frac{1}{T_{do}^{'}}\left[E_{fd} - e_q\right] \tag{2}$$

$$\dot{E}_{fd} = -\frac{1}{T_A}\left(E_{fd} - E_{fdo}\right) + \frac{K_A}{T_A}\left(V_{to} - V_t\right)$$

$$\dot{V}_{dc} = \frac{e}{C_{DC}}\left[I_{lod}\cos\psi + I_{loq}\sin\psi\right]$$

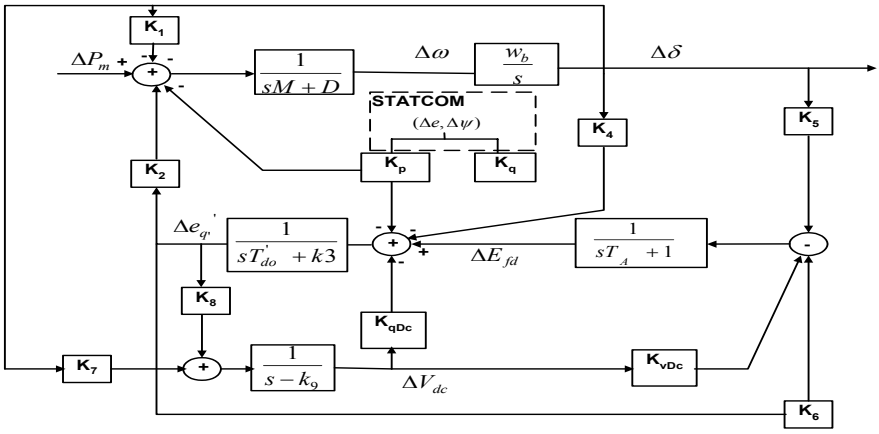

Fig.2 Block diagram of the linearized system with STATCOM

The symbols used are given in the Nomenclature. Expressions for e_q in terms of transmission line current along direct axis I_{tLd}, the power output P_e, and terminal voltage V_t are obtained in terms of system states, and then (2) is linearized to give,

$$\dot{x} = Ax + Bu \tag{3}$$

Here, x is the vector of the states $[\Delta\delta \;\; \Delta\omega \;\; \Delta e_q^{'} \;\; \Delta E_{fd} \;\; \Delta V_{DC}]$ and the control vector u comprises of $[\Delta e \;\; \Delta\psi]$. Fig. 2 shows the block diagram for the linearized system. The coefficients K_1, K_2, …. etc. used in the diagram are given in the Appendix.

Top

3. SIMULATION RESULTS WITH PID CONTROLLER

It has been reported that control in the STATCOM phase angle loop alone is not effective in providing the damping to the power system but its presence is necessary in stabilizing the overall system voltage [Wang, 1999]. The effectiveness of STATCOM magnitude control strategy is tested by applying different combinations of PID controls. A gain of unity is considered in the magnitude control loop. A 100% input torque pulse for 0.05 sec. was used to simulate the disturbance. Fig. 3 shows the rotor angle variations of the generator for the following cases, a) proportional control, b) PD control, c) PI control, and d) PID control. The study of the dynamic model indicates that suitably designed PID controller can enhance electromechanical damping of the system. However, variations in the electrical transients such as STATCOM bus voltage, controller current outputs etc. are, generally, larger. The other difficulty with the PID controller is that the gains need to be retuned for various operating conditions. Therefore, a robust design procedure for the STATCOM voltage magnitude control has been considered to overcome the difficulty of the PID controller.

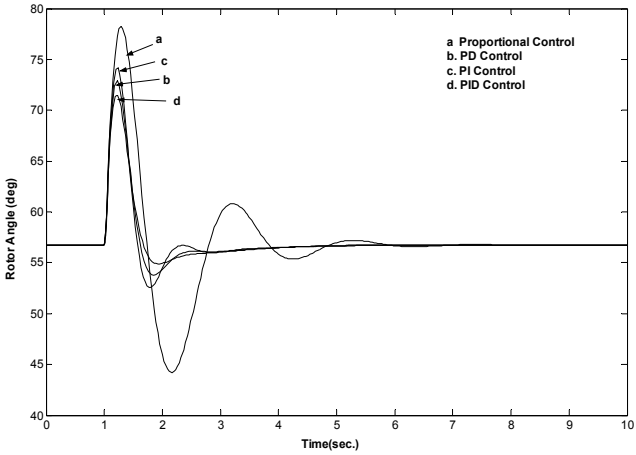

Fig.3 Comparison of generator rotor angle variations with different gains of PID controller.

4. ROBUST CONTROL DESIGN

A robust controller is designed for a range of operating conditions by considering perturbations around a nominal plant. These perturbations are modeled as multiplicative uncertainties in the design procedure. This section gives a brief theory of the uncertainty model, the robust stability criterion, and a graphical technique termed 'loop-shaping' that is employed to design the robust controller. Finally, an algorithm for the control design is presented.

4.1 Uncertainty Modeling

For a nominal plant transfer function *P*, the perturbed functions, $\tilde{P}$ because of the variations of operating conditions, can be expressed as,

$$\tilde{P} = (1 + \Theta W_2)P \tag{4}$$

Here, W_2 is a fixed stable transfer function, the weight, and Θ is a variable transfer function satisfying $\|\Theta\|_\infty < 1$. $\|\Theta\|_\infty$ is the upper bound on the value of Θ. In the multiplicative uncertainty model (4), ΘW_2 is the normalized plant transfer function away from 1. If $\|\Theta\|_\infty < 1$, then,

$$\left| \frac{\tilde{P}(j\omega)}{P(j\omega)} - 1 \right| \le |W_2(j\omega)|, \forall \omega \tag{5}$$

This implies that $|W_2(j\omega)|$ provides the uncertainty profile, and is the upper boundary of all the normalized plant transfer function away from 1 in the frequency plane.

4.2. Robust Stability and Performance

Consider a multi-input control system given in Fig. 4. Suppose that the plant transfer function P belongs to set a **P.** A controller C provides stability iff it provides internal stability for every plant in the set **P**.

Theorems: *C provides robust stability iff* $\|W_2 T\|_\infty < 1$ *for multiplicative uncertainty. Also, a necessary and sufficient condition for robust performance is* $\| |W_1 S| + |W_2 T| \|_\infty < 1$. *The nominal performance condition is given as* $\|W_1 S\|_\infty < 1$ [Doyle et al, 1992].

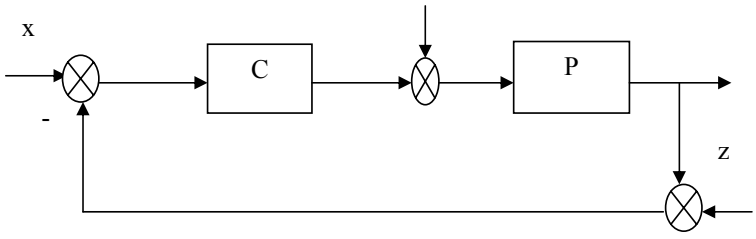

Fig.4 Unity feedback plant with controller.

In the above W_1 is a real, rational, stable and minimum phase function. *T* is the input-output transfer function, complement of the sensitivity function *S,* and is given as

$$T = 1 - S = \frac{1}{1+L} = \frac{1}{1+PC} \tag{6}$$

4.3 Loop-Shaping Technique

Loop-shaping is a graphical procedure to design a proper controller C satisfying robust stability and performance criteria given in sec. 4.2. The basic idea of the method is to construct the loop transfer function, *L=PC* to satisfy the robust performance criterion approximately, and then to obtain the controller from the relationship *C=L/P*. Internal stability of the plants and properness of *C* constitute the constraints of the method. Conditions on L are such that *PC* should not have any cancellation of unstable poles of P. A necessary condition for robustness is that either or both $|W_1|$, $|W_2|$ must be less then 1 [Levine, 1996]. If we select a monotonically decreasing W_1 satisfying the other constraints on it, it can be shown that at low frequency the open-loop transfer function *L* should satisfy,

$$|L| > \frac{|W_1|}{1-|W_2|} \tag{7}$$

while, for high frequency

$$|L| < \frac{1-|W_1|}{|W_2|} \approx \frac{1}{|W_2|} \tag{8}$$

At high frequency $|L|$ should roll-off at least as quickly as $|P|$ does. This ensures properness of C. The general feature of open loop transfer function is that the gain at low frequency should be large enough, and $|L|$ should not drop–off too quickly near the crossover frequency to avoid internal instability.

4.4 The Algorithm

The control design procedure for robust stability and robust performance can be summarized in the following steps.

1. Obtain the dB-magnitude plot for the nominal as well as perturbed plant transfer functions.
2. Construct W_2 satisfying constraint (5).
3. Select W_1 as a monotonically decreasing real, rational and stable functions

4. Choose L such that it satisfies conditions (7) and (8). The transition at crossover frequency should not be at a slope steeper than –20dB/decade.
5. Check for the nominal and robust performance criteria given in the theorems in section 4.2.
6. Test for internal stability by direct simulation of the closed loop transfer function for pre-selected disturbances or inputs.
7. Repeat steps 4 through 6 until satisfactory L and C are obtained.

5. IMPLEMENTATION

The robust controller design procedure starts by arranging the system in the form shown in Fig. 4. The collapsed block diagram for the magnitude control only is shown in Fig. 5. Here C_e represents robust controller for the magnitude control 'e'. P is the plant transfer function $C(sI-A)^{-1}B$. C is selected such that $\Delta\omega$ is the plant output.

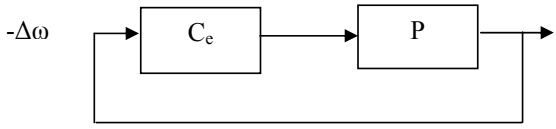

Fig.5 Collapsed block diagram for robust magnitude controller.

The nominal operating point for the design was computed for a delivered power of 0.9 at unity power factor load. Off-nominal power outputs between 0.8 pu to 1.4 pu and power factor from 0.8 lagging to 0.8 leading were considered. The dB magnitude vs. frequency response for the nominal and perturbed plants is shown in Fig. 6.

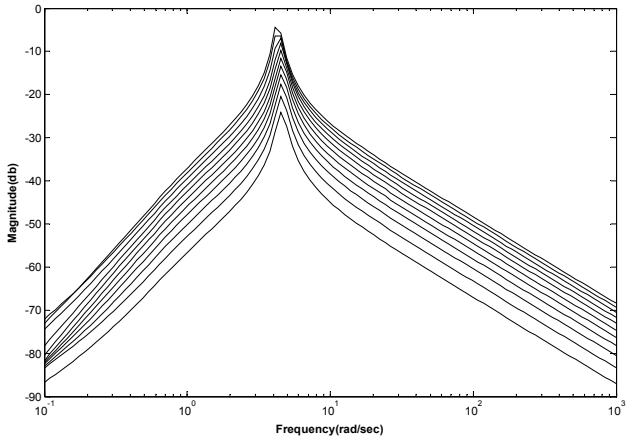

Fig.6 Nominal and perturbed plant transfer functions for robust control design

The nominal plant transfer function for the selected operating point is computed as,

$$P = \frac{0.2466\, s^2 (s + 100.774)(s - 0.214309)}{(s + 99.1923)(s + 1.0901)(s + 0.0527)(s^2 + 0.65484\, s + 21.4956)} \tag{9}$$

From Fig.6, the quantity $|\tilde{P}(j\omega) / P(j\omega) - 1|$ for each perturbed plant is constructed and the uncertainty profile is fitted to the following function,

$$W_2(s) = \frac{2.165\, s^2 + 4.221\, s + 27.44}{2.5 s^2 + 2.436\, s + 18.92} \tag{10}$$

A butterworth filter satisfies all the properties for $W_1(s)$ and is written as

$$W_1(s) = \frac{K_d f_c^2}{s^3 + 2 s^2 f_c + 2 s f_c^2 + f_c^3} \tag{11}$$

For $K_d = 0.01$ and $f_c = 1$, and for a choice of open loop transfer function L as,

$$L = \frac{0.5(s + 0.009)(s + 100.774)(s - 0.214309)(s + 1)}{(s + 12)(s + 0.0901)(s + 0.01)(s^2 + 0.65484\, s + 21.4956)} \tag{12}$$

gives the desired controller transfer function,

$$C_e = \frac{2.0273\,(s + 1)(s + 1.0901)(s + 0.0527)(s + 0.009)(s + 99.1923)}{s^2 (s + 12)(s + 0.090)(s + 0.01)} \tag{13}$$

The db-magnitude plots relating W_1, W_2 and L, which were employed to arrive at this controller, is shown in Fig. 7. The plots for the nominal performance and robust performance criteria are shown in Fig 8. As shown in the figure, both nominal and robust performance criteria were well satisfied.

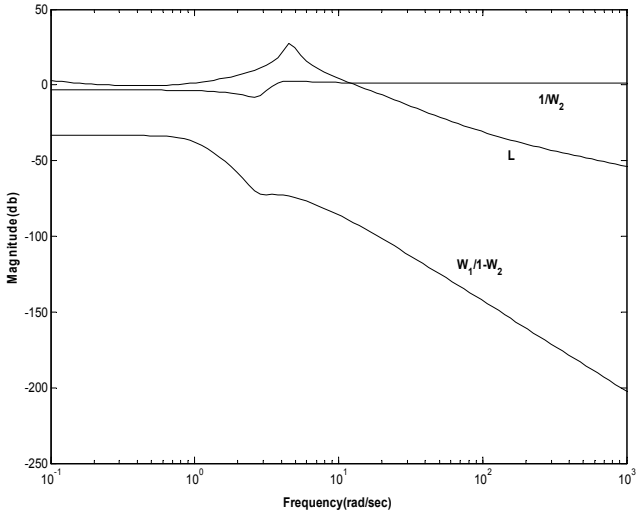

Fig. 7 Loop-shaping plots relating W_1, W_2 and L

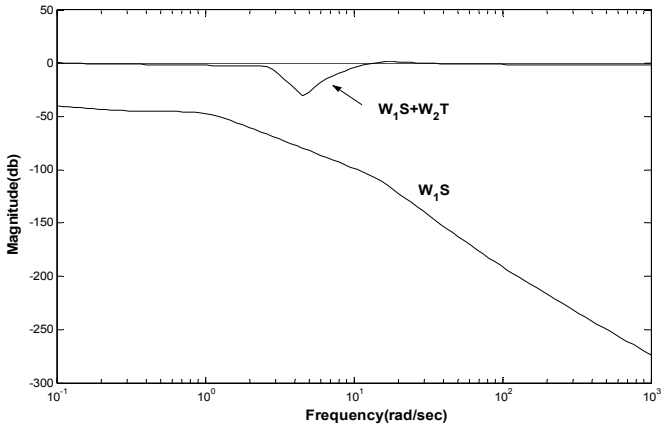

Fig.8 The nominal and robust performance criteria.

The robust STATCOM controller was tested by applying an input torque pulse of 100% for 0.05 sec. duration to the generator shaft. The simulations results obtained for a number of operating conditions are shown in Fig. 9 and 10. Fig. 9 shows the rotor angle variation for the following operating conditions, a) nominal operating condition b) unity power output at 0.95 lagging power factor, and c) 0.5 pu at 0.95 lag and d) 1.2 pu at 0.98 lead. It was observed that the designed magnitude control provides good damping for all operating conditions. Expectedly, the response of the states far away from the nominal is not as good. This is exhibited by a slightly oscillatory response for 0.5 pu loading shown by curve c.

Fig. 10 shows the corresponding variations in the mid-bus voltage. The robust controller maintains the bus voltage to its desired value faithfully. The maximum transient overshoot was observed to be about 17% for a very heavy loading condition.

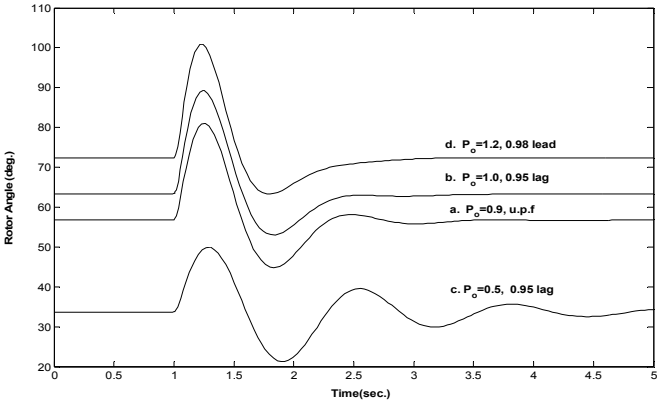

Fig.9 Rotor angle with robust control of voltage magnitude.

Top

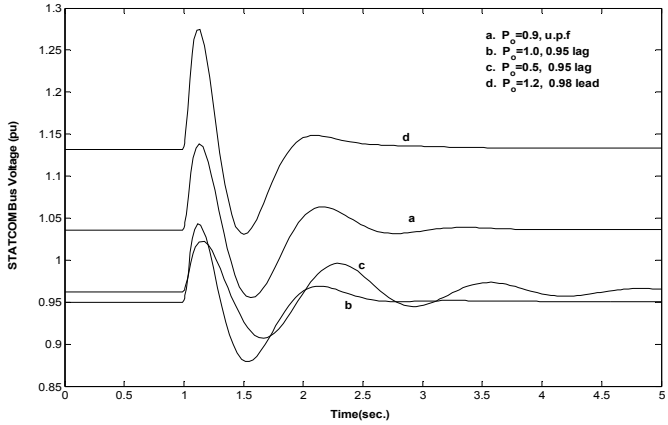

Fig.10 STATCOM bus voltage corresponding to Fig. 9.

The robust controller designed was also tested for a three-phase fault for 0.1 sec. duration at the infinite bus of the power system. Figs. 11 and 12 show the generator rotor angle and STATCOM bus voltage variations for a wide range of power output conditions. Similar loading conditions as the torque pulse disturbance condition were considered. These are, a) nominal operating condition, b) unity power output at 0.95 lagging power factor, c) 0.5 pu power at 0.95 lag power factor, and d) 1.2 pu power at 0.98 lead power factor. Results show that the robust strategy controls the electromechanical and electrical transients very effectively. Even for large disturbances of 0.15 second duration fault, the robust controller is able to stabilize the system. The voltage variations, however, are large in this case.

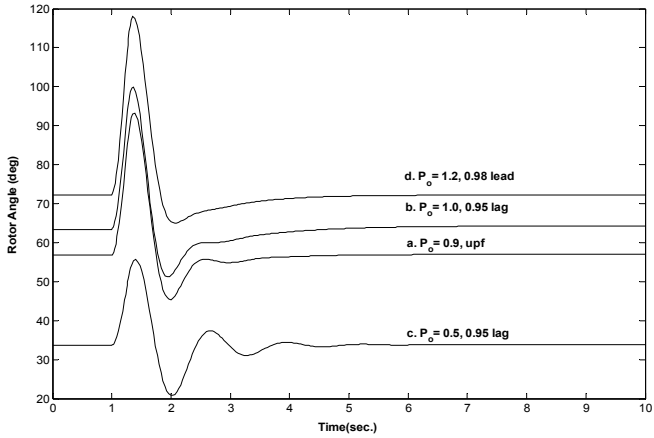

Fig.11 Rotor angle variations with robust controller for three- phase fault at infinite bus.

Top

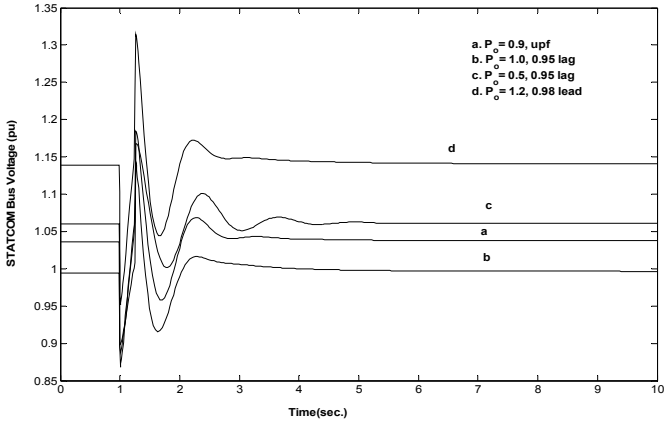

Fig.12 STATCOM bus voltage variations corresponding to Fig. 11.

6. CONCLUSION

A comparative study has been carried out for different PID controls applied in the voltage magnitude control loop of a STATCOM. It has been found that the gain settings of the PID controller need to be retuned for the varying operating conditions. A robust controller for the magnitude control has been designed by using loop-shaping technique. The designed controller has been tested for a number of operating conditions including three-phase faults. The robust design was found to be very effective in providing damping to the system. The operating conditions for which the controller performs well, however, depend on the proximity of the perturbed plants from the nominal ones.

NOMENCLATURE

X	Transmission line reactance
M, D	Inertia and damping coefficients
V_t	Machine terminal voltage
P_m, P_e	Machine input and output power
φ	Phase Angle of the mid-bus voltage
e_q', e_q	Internal voltage behind transient and synchronous reactances
E_{fd}	Generator field voltage
δ	Generator rotor angle
T_{do}'	open circuit field time constant
K_A', T_A'	Exciter gain and time constants
x_d , x_d'	Direct axis synchronous and transient reactance

ω_o	Base radian frequency
i_d, i_q	Armature d-q currents
v_d, v_q	Armature d-q voltage
V_b, V_m	Infinite bus and STATCOM voltages

REFERENCES

1. Doyle, J.C., Francis, B.A. and Tannenbaum, A.R., 1992, Feedback Control Theory. McMillan Publishing Co., New York.
2. Gyugi, L., 1994, "Dynamic compensation of AC transmission line by solid-state synchronous voltage sources", *IEEE Transactions on Power Delivery*, 9(2), pp. 904-911.
3. Li, C., Q. Jiang, Z. Wang and D. Retzmann, 1998, "Design of Rule Based Controller for STATCOM", *Proc. Of 24th Annual Conf. Of IEEE Ind. Electronics Society IECON. '98,* pp. 467-472.
4. Machowaski, J., 1997, Power System Dynamics and Stability. John Wiley and Sons.
5. Levine, W.S., 1996, The Control Handbook. CRC Press and IEEE Press.
6. Padiyar, K.R. and Kulkarni, A.M., 1996, "Analysis & design of voltage control of Static Condenser" *IEEE Conf. On Power Electronics Derives & Energy System for Industrial Growth,* 1, pp. 393-398.
7. Wang, H.F., 1999, "Phillips-Heffron model of power systems installed with STATCOM and applications" *IEE proc.-Gener. Transm. Distrib.,* 146(5), pp. 521-527.
8. Wang, H.F. and Li, F., 2000, "Design of STATCOM Multivariable Sampled Regulator" *Int. Conf. On Electronic utility Deregulation and Power-tech. 2000, City University of London,* April 2000.

APPENDIX

Breaking the voltages and currents along the d-q axes, the expressions for power output and terminal voltage are written as,

$$
\begin{aligned}
P_e &= v_d I_{tLd} + I_{tLq} = e_q^{'} I_{tLd} + \left(x_d - x_d^{'}\right) I_{tLq} \\
V_t &= \sqrt{v_d^2 + v_q^2} = \sqrt{\left(e_q^{'} - x_d^{'} I_{tLd}\right)^2 + x_q^{'} I_{tLq}{}^2} \\
e_q &= e_q^{'} + (x_d - x_d^{'}) I_{tLd}
\end{aligned}
\qquad \text{(A.1)}
$$

Top

The expressions for transmission line currents in terms of states are,

$$I_{tLd} = \frac{\left(1+\frac{X_{LB}}{X_{SDT}}\right)e_q' - \frac{X_{LB}}{X_{SDT}}eV_{DC}\sin\psi - V_B\cos\delta}{X_{tL}+X_{LB}+\frac{X_{TL}}{X_{LB}}+\left(1+\frac{X_{LB}}{X_{SDT}}\right)x_d'}$$

$$I_{tLq} = \frac{\frac{X_{LB}}{X_{SDT}}eV_{DC}\cos\psi + V_B\sin\delta}{X_{tL}+X_{LB}+\frac{X_{TL}}{X_{LB}}+\left(1+\frac{X_{LB}}{X_{SDT}}\right)x_q'} \qquad \text{(A.2)}$$

The STATCOM currents are,

$$\bar{I}_{lod} = \frac{e_q'}{X_{SDT}} - \frac{\left(x_d' + X_{tL}\right)I_{tlq}}{X_{SDT}} - \frac{eV_{DC}\sin\psi}{X_{SDT}}$$

$$\bar{I}_{loq} = \frac{eV_{DC}\cos\psi}{X_{SDT}} - \frac{\left(x_q' + X_{tL}\right)I_{tlq}}{X_{SDT}} \qquad \text{(A.3)}$$

The linearized system of state equations is,

$$\begin{aligned}
\Delta\dot{\delta} &= \omega_o\Delta\omega \\
\Delta\dot{\omega} &= -\frac{1}{M}\left[-\Delta P_e - D\Delta\omega\right] \\
\Delta\dot{e}_q' &= \frac{1}{T_{do}'}\left[-\Delta e_q' + \Delta E_{fd} - \left(x_d - x_d'\right)\Delta I_{tLd}\right] \\
\Delta\dot{E}_{fd} &= -\frac{1}{T_A}\left(\Delta E_{fd} - K_A\Delta V_t\right) \\
\Delta\dot{V}_{dc} &= \frac{1}{C_{Dc}}\left[\begin{array}{l}\left(I_{lodo}\cos\psi_o + I_{loqo}\sin\psi_o\right)\Delta e \\ + e_o\left(-I_{lodo}\sin\psi_o + I_{loqo}\cos\psi_o\right)\Delta\psi + \\ + e_o\left(\cos\psi_o\,\Delta I_{lodo} + \Delta I_{loqo}\sin\psi_o\right)\end{array}\right]
\end{aligned} \qquad \text{(A.4)}$$

where,

$$\begin{aligned}
\Delta P_e &= K_1\Delta\delta + K_2\Delta e_q' + K_{pDC}\Delta V_{DC} + K_{pe}\Delta e + K_{p\psi}\Delta\psi \\
\Delta e_q &= K_4\Delta\delta + K_3\Delta e_q' + K_{qDC}\Delta V_{DC} + K_{qe}\Delta e + K_{q\psi}\Delta\psi \\
\Delta V_t &= K_5\Delta\delta + K_6\Delta e_q' + K_{vDC}\Delta V_{DC} + K_{ve}\Delta e + K_{v\psi}\Delta\psi
\end{aligned} \qquad \text{(A5)}$$

Top